

## Measurement of oblique-incidence absorption coefficients of various types of absorbing materials in a thin chamber

Tetsuya SAKUMA<sup>1</sup>; Naohisa INOUE<sup>2</sup>; Yuta SAKAYOSHI<sup>3</sup>

<sup>1</sup>The University of Tokyo, Japan

<sup>2</sup>The University of Tokyo, Japan

<sup>3</sup>Nippon Sheet Glass Environment Amenity Co., Ltd, Japan

### ABSTRACT

A novel measurement system for oblique-incidence absorption coefficients has been developed using a thin rectangular chamber and two arrays of microphones. In this method, a series of incident and reflected plane waves at corresponding angles are decomposed based on a propagation mode expansion technique. Accordingly, absorption coefficients are determined at discrete incidence angles, of which number increases with frequency. First, a test measurement for glass wool was done in comparison with theoretical estimates. As a result, the measurement system was basically validated, but abnormal values were occasionally observed at singular combinations of frequency and incidence angle. The faults theoretically occur under two conditions: the interval of microphone arrays coincides with a half wavelength in incidence angle, and some modes are not generated due to loudspeaker position mismatch. Therefore, two post-processes were incorporated to exclude abnormal values systematically. Then, measurements were done for various types of absorbing materials, such as urethane foam, rock wool board, perforated panel, and honeycomb resonators, and their incidence angle dependence of absorption coefficients was examined.

Keywords: Absorption coefficient, Oblique incidence, Mode expansion

### 1. INTRODUCTION

There exist several methods for measuring oblique-incidence sound absorption coefficients in the free or semi-free field, which generally requires a specimen with a large surface area [1-3]. On the other hand, we have recently proposed a novel method where the measurement is done for a strip of specimen in a thin rectangular chamber, and applying a propagation mode expansion technique with two arrays of microphones [4]. In the thin-chamber method, a series of incident and reflected plane waves at corresponding angles are decomposed in the two-dimensional field, which is similar to the impedance tube method for measuring normal-incidence absorption coefficients. Accordingly, normal- and oblique-incidence absorption coefficients can be determined at a series of incidence angles corresponding to the propagation modes, of which number increases with frequency. However, some faults can theoretically occur under two singular conditions: the interval of microphone arrays coincides with a half wavelength in incidence angle, and some modes are not excited due to loudspeaker position mismatch.

In the first part of this paper, a test measurement is done for glass wool to validate the measurement system in comparison with theoretical estimates, where two post-processes are incorporated to exclude abnormal values systematically under the two unsuitable conditions. Furthermore, using the measured values at all the combinations of frequency and incidence angle, oblique-incidence absorption coefficients at 1/3-octave bands are estimated by the least squares method. In the latter part, measurements are done for various types of absorbing materials, such as urethane foam, rock wool board, perforated panel, and honeycomb resonators. In comparison with theoretical estimates, their incidence angle dependence of absorption coefficient is examined.

<sup>1</sup> sakuma@k.u-tokyo.ac.jp

<sup>2</sup> inoue@env-acoust.k.u-tokyo.ac.jp

<sup>3</sup> Yuta.Sakayoshi@nsg.com

## 2. MEASUREMENT METHOD AND SYSTEM

### 2.1 Measurement Principle

Considering a two-dimensional sound field with rigid boundary conditions at  $x=0$  and  $x=W$  (Fig. 1), sound pressure is expressed as the superposition of propagation modes, that is,

$$p(x,y) = \sum_{n=0}^{\infty} [a_n \exp(-jk_y^n y) + b_n \exp(jk_y^n y)] \cos(jk_x^n x), \quad (1)$$

where  $k_x^n$  and  $k_y^n$  are  $n$ th wave numbers in  $x$  and  $y$  directions. The  $n$ th mode satisfies  $k_x^n = n\pi/W$  and  $k_y^n = \sqrt{k^2 - k_x^{n2}}$ , thus its traveling angle is defined as

$$\theta_n = \arcsin\left(\frac{k_x^n}{k}\right) = \arcsin\left(\frac{nc}{2Wf}\right). \quad (2)$$

Supposing that the surface of a specimen is at  $y=0$ ,  $a_n$  and  $b_n$  are the amplitudes of the incident and reflected plane waves, respectively. Accordingly, the oblique-incidence absorption coefficient at the incidence angle  $\theta_n$  is given by  $\alpha_n = 1 - |b_n/a_n|^2$ .

Multiplying Eq. (1) by  $m$ th  $x$ -directional basis,  $\cos(jk_x^m x)$ , and integrating it over  $x$  axis can extract the average sound pressure for  $m$ th propagation mode as follows:

$$\bar{p}_m(y) = \frac{\varepsilon_m}{W} \int_0^W p(x,y) \cos(jk_x^m x) dx = a_m \exp(-jk_y^m y) + b_m \exp(jk_y^m y), \quad (3)$$

where  $\varepsilon_m$  is 1 for  $m=0$ , and 2 for  $m>0$ . In the measurement, sound pressures are measured in the lines  $y_1$  and  $y_2$ , and then,  $\bar{p}_m$  are calculated for each mode at the two lines. Finally, the amplitudes of the incident and reflected waves of each mode can be determined by

$$\begin{Bmatrix} a_m \\ b_m \end{Bmatrix} = \frac{1}{2j \sin(k_y^m \Delta y)} \begin{bmatrix} \exp(jk_y^m y_2) & -\exp(jk_y^m y_1) \\ -\exp(-jk_y^m y_2) & \exp(-jk_y^m y_1) \end{bmatrix} \begin{Bmatrix} \bar{p}_m(y_1) \\ \bar{p}_m(y_2) \end{Bmatrix}, \quad (4)$$

provided that  $k_y^m \Delta y \neq n\pi$  where  $\Delta y = y_2 - y_1$ .

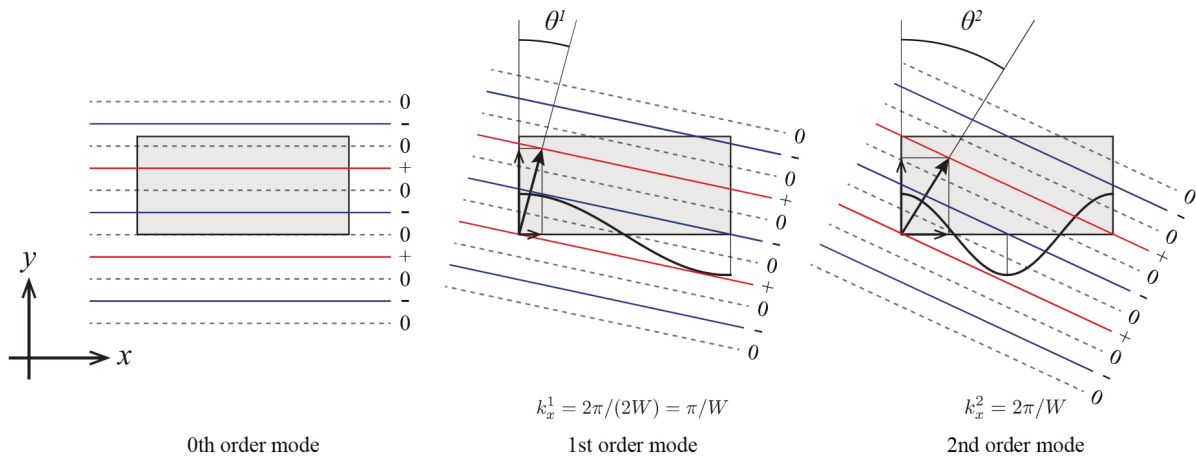


Figure 1 – Propagation modes in two-dimensional sound field.

### 2.2 Measurement System

Figure 2 shows the geometry of a thin chamber with dimensions of  $W = 1.3$  m,  $D = 0.6$  m, and  $H = 0.05$  m, where a strip of specimen is installed along a long side. A loudspeaker can be installed at one of 10 positions on the opposite side to a specimen, and the position near a corner (no.10) is chosen in order to generate all propagation modes. The interval of two lines for microphone arrays is 8 cm, and 64 receiving points are located at an interval of 2 cm in each line. In actual, changing two circular holders with 4 microphones, 8ch impulse response measurements using a 1.37-second log swept sine signal are done in turn. Subsequently, complex sound pressures are calculated at all points by the Fourier transform, and the average sound pressures of each propagation mode are calculated at the two receiving lines using the trapezoidal rule in Eq. (3).

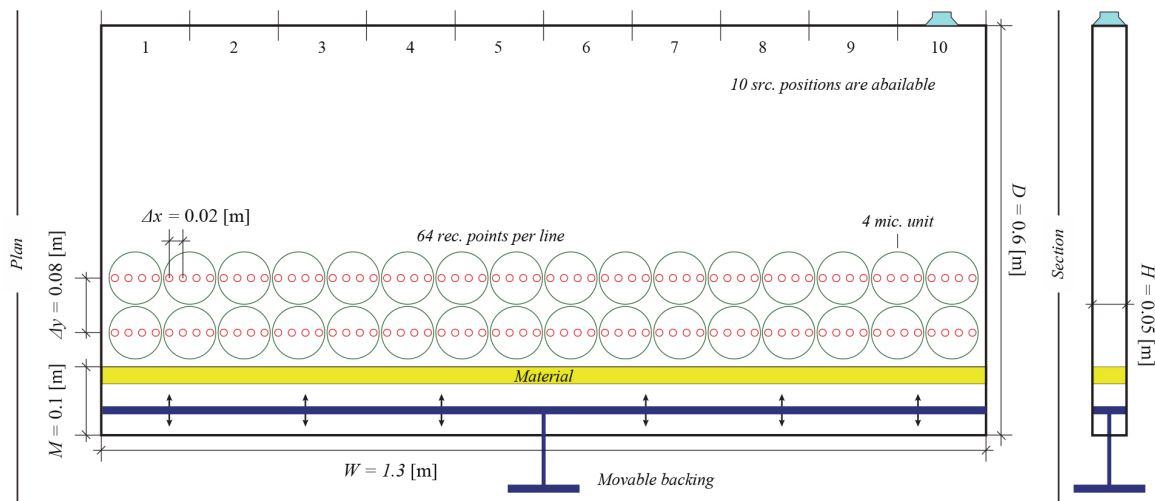


Figure 2 – Geometry of the thin chamber with two microphone arrays and a loudspeaker.

### 2.3 Measurable Frequency Range and Angles

The above thin-chamber system has limitations on frequency and incidence angle in the measurement. First, because of the requirement for two-dimensional field, the height of the chamber gives the upper limit frequency,  $f_u = c/2H$ , which is 3.4 kHz for this chamber. Second, the incident and reflected waves cannot be determined by Eq. (4) under the condition,  $k_y^m \Delta y = \pi$ , where the interval of microphone arrays coincides with a half wavelength in incidence angle. The singular frequency for each mode is expressed by

$$f_s^m = \frac{c}{2} \sqrt{\left(\frac{m}{W}\right)^2 + \frac{1}{\Delta y^2}}. \quad (5)$$

Therefore, measurement faults possibly occur at specific incidence angles above the lowest singular frequency,  $f_s^0 = c/2\Delta y$ , which is 2.1 kHz for this chamber. If avoiding the faults under  $f_u$ , the interval of microphone arrays should be set less than the height of chamber, in a similar manner to the impedance tube method. Figure 3 shows the measurable frequency range and incidence angles in this chamber, where the number of propagation modes increases with frequency. For instance, the 1/3-octave band of 500 Hz contains 4 oblique-incidence modes and a normal-incidence mode, which could be enough to estimate the incidence angle dependence of absorption coefficient.

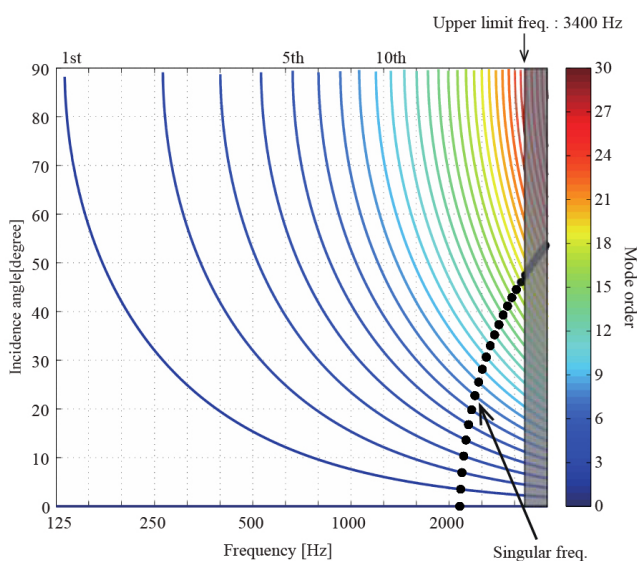


Figure 3 – Measurable frequency range and incidence angles in the chamber.

### 3. VALIDATION OF THE MEASUREMENT SYSTEM

A test measurement of oblique-incidence absorption coefficients is done for glass wool with a bulk density of  $32 \text{ kg/m}^3$  and a thickness of 25 mm. First, two post-processes are examined for excluding outliers due to the interval of microphone arrays and loudspeaker position mismatch, respectively. Subsequently, using the measured values, oblique-incidence absorption coefficients at 1/3-octave bands are estimated by the least squared method.

#### 3.1 Treatment for Singular Frequencies

Figure 4 (a) shows the oblique-incidence absorption coefficients of the glass wool, measured in the 1/3-octave band of 2000 Hz. As is illustrated in Fig. 3, this band includes singular frequencies due to the interval of microphone arrays, thus causing abnormal values between 0 and 20 degrees. Therefore, a post-process for excluding the outliers is introduced, where measured values are removed if  $k_y^m \Delta y$  is within  $(1 \pm \Delta)\pi$ . Figures 4 (b), (c) and (d) show the results after the post-process with  $\Delta = 0.01, 0.05$  and  $0.1$ . It is seen that the outliers below 20 degrees steadily disappear with increasing  $\Delta$ , however, those around 40 degrees still remain. In the following,  $\Delta$  is fixed at 0.1 for this post-process.

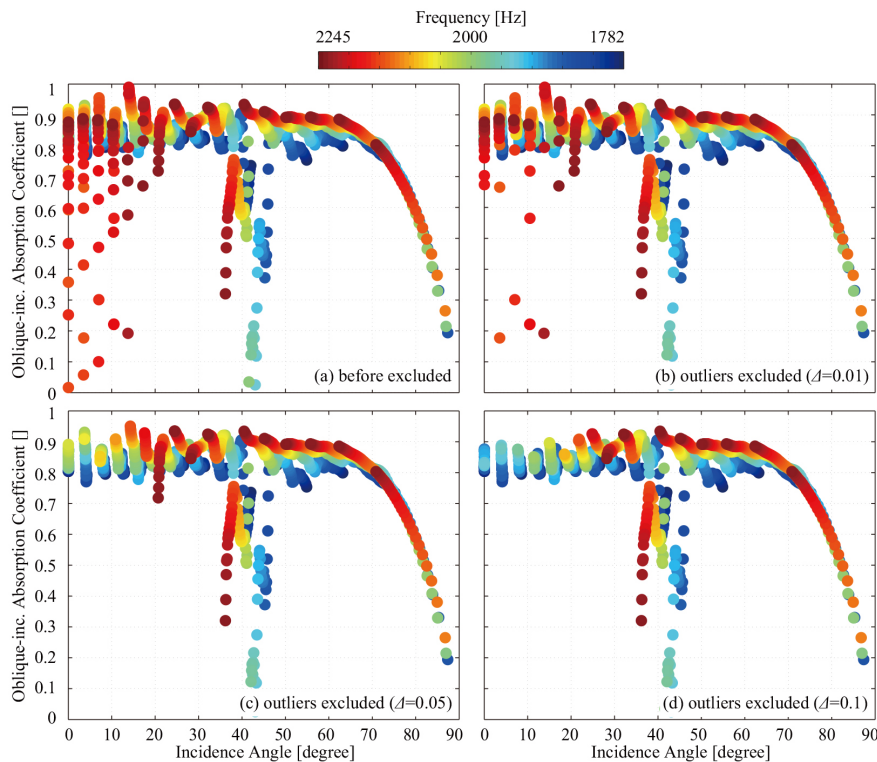


Figure 4 – Oblique-incidence absorption coefficients measured in 1/3-octave band of 2000 Hz: (a) raw, and (b) processed with  $\Delta = 0.01$ , (c)  $\Delta = 0.05$ , (d)  $\Delta = 0.1$ .

#### 3.2 Treatment for Unexcited Modes

Figure 5 shows the relative sound pressure levels of incident and reflected plane waves decomposed for calculating the absorption coefficients in Fig. 4 (a). It is seen that the levels of incident waves remarkably drop around 40 degrees, which is considered to result in the remaining outliers in Fig. 4 (d). Figure 6 illustrates the positional relation of the loudspeaker position (no.10) with the three propagation modes (9th, 10th and 11th). In theory, the 10th mode cannot be excited, and there is a possibility that the two adjacent modes will be not sufficiently excited. Therefore, another post-process for excluding unexcited modes is additionally introduced, where measured values are removed if the amplitude of incidence wave is less than  $\Gamma$  times the average amplitude over all modes. Figure 7 shows the results before and after the second post-process with  $\Gamma = 1/4, 1/2$  and  $3/4$ . It is seen that the outliers after the first post-process are sufficiently excluded with  $\Gamma = 1/2$  (-6 dB relative to the average level), thus this criterion is used in the following.

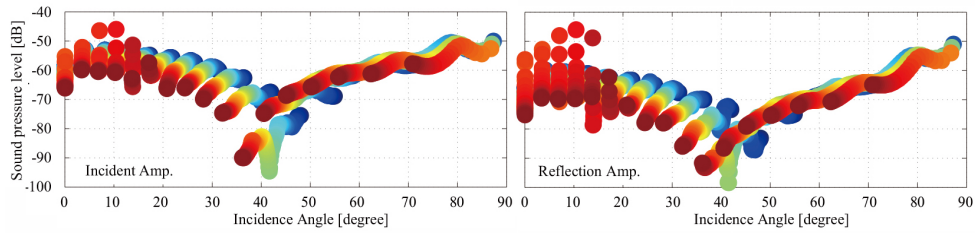


Figure 5 – Relative sound pressure level of incident and reflected waves in 1/3-octave band of 2000 Hz.

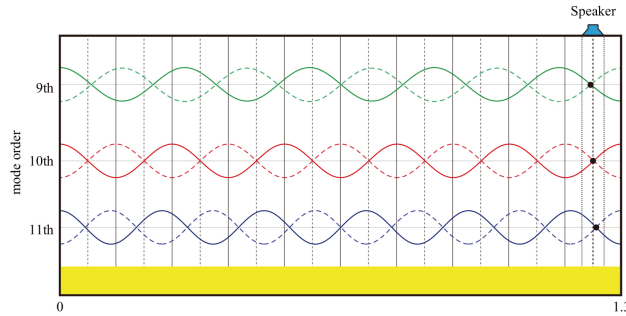


Figure 6 – Loudspeaker position mismatch for three propagation modes.

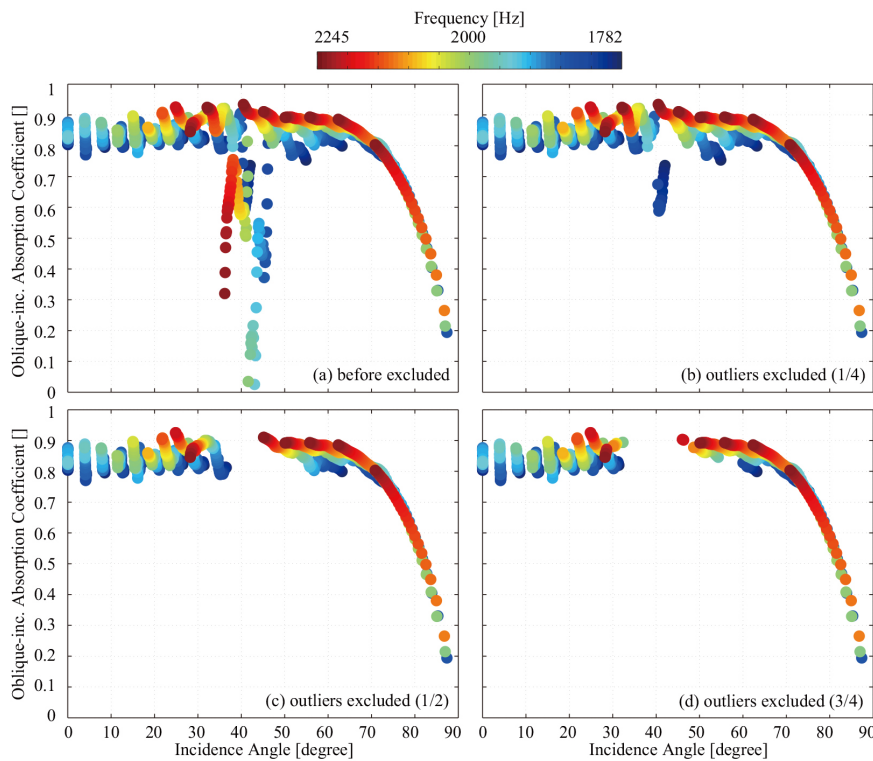


Figure 7 – Oblique-incidence absorption coefficients measured in 1/3-octave band of 2000 Hz: (a) before the second process, and (b) processed with  $\Gamma = 1/4$ , (c)  $\Gamma = 1/2$ , (d)  $\Gamma = 3/4$ .

### 3.3 Estimation of Incidence Angle Dependence

Figure 8 (a) shows the measured values at the center frequency of each 1/3-octave band, but which are insufficient and uncertain to estimate the incidence angle dependence of absorption coefficient over all angles. On the other hands, Fig. 8 (b), (c) and (d) show the measured values at all combinations of frequency and incidence angle in the three bands, which will be useful to estimate the incidence angle dependence in each band. Accordingly, estimations using all the measured values excluding outliers are tested with two different curve fittings using the least squares method. One is a global fitting with a high-order polynomial, and another is a piecewise estimation where lower-order

polynomials are used for the three angle ranges divided at 60 and 85 degrees. In the two fittings, the absorption coefficient at 90 degrees is assumed to be zero, and the continuity of slope is imposed at the two dividing angles in the piecewise fitting.

Figure 9 shows the absorption coefficients of glass wool with thicknesses of 25 and 50 mm, estimated by the two curve fittings at 500, 1000 and 2000 Hz, where 5th-order polynomials are used in the global fitting, while for the piecewise estimation, 2nd-, 4th- and 1st-order polynomials are used below 60 degrees, between 60 and 85 degrees, and above 85 degrees, respectively. In addition, theoretical lines are indicated, which are calculated with some parameters that are estimated from normal-incidence absorption coefficients based on Kato model [5]. It is seen that the estimated results with the two fittings are generally in good agreement with the theoretical ones, although the estimates tend to be greater around 70 degrees, especially at 500 Hz. Moreover, small unnatural fluctuations appear below 60 degrees in the results with the global estimation, so that, the piecewise estimation may be more suitable for this purpose. Finally, the feasibility of the developed measurement system is validated in the case with glass wool.

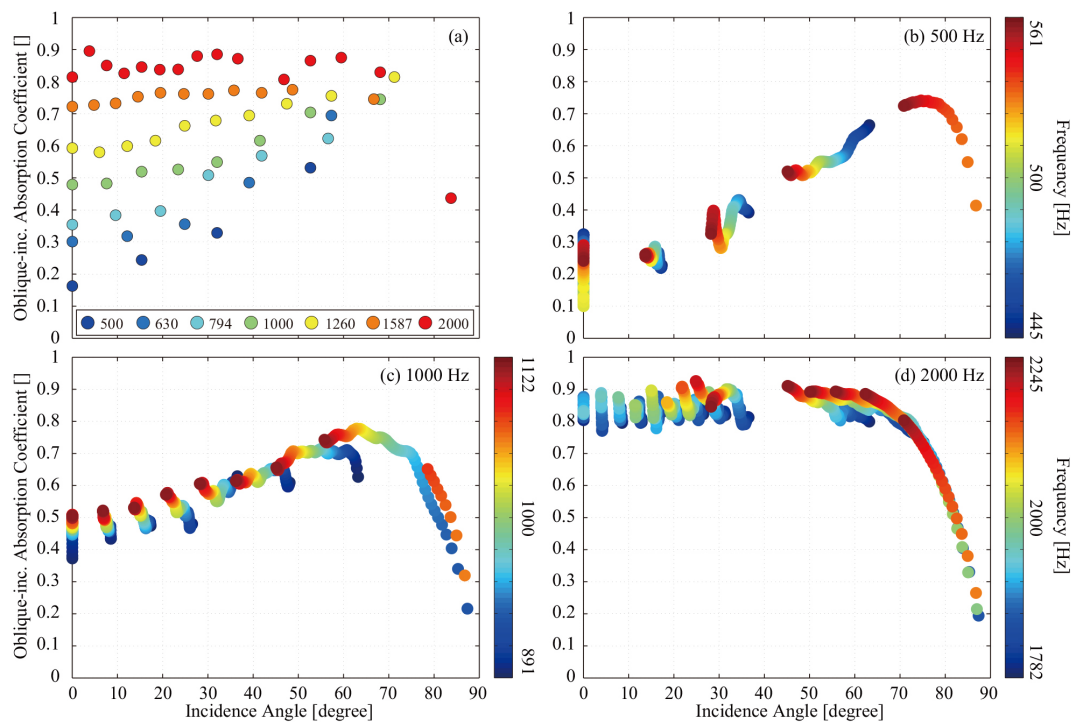


Figure 8 – Oblique-incidence absorption coefficients measured in 1/3-octave bands: (a) center frequencies, (b) 500 Hz band, (c) 1000 Hz band, (d) 2000 Hz band.

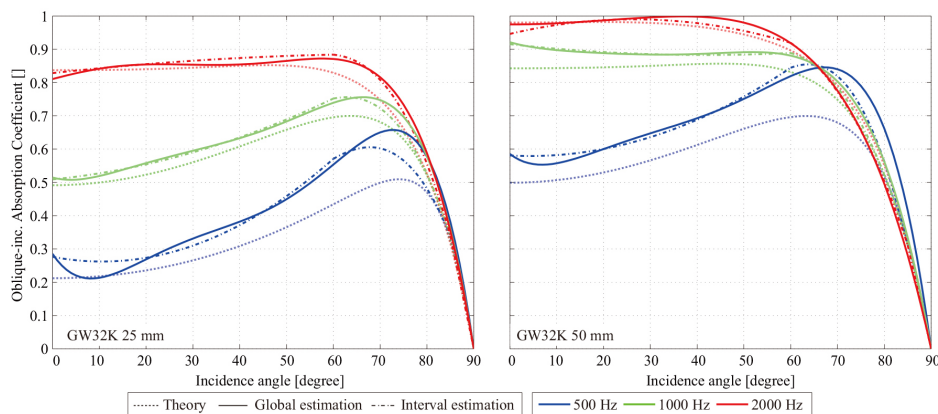


Figure 9 – Incidence angle dependence of glass wool ( $32 \text{ kg/m}^3$ ) with a thickness of (a) 25 mm, (b) 50 mm, estimated by two curve fittings and by theory at 500, 1000 and 2000 Hz:

## 4. MEASUREMENTS FOR VARIOUS ABSORBING MATERIALS

### 4.1 Porous Materials

Measurements of oblique-incidence absorption coefficients are done for three types of porous materials with different bulk densities and thicknesses: a glass wool ( $\rho_b = 32 \text{ kg/m}^3$ ,  $t = 25 \text{ mm}$ ), an urethane foam ( $\rho_b = 24 \text{ kg/m}^3$ ,  $t = 25 \text{ mm}$ ), and a rock wool board ( $\rho_b = 325 \text{ kg/m}^3$ ,  $t = 9 \text{ mm}$ ). Figure 10 shows the measured values excluding outliers in the 1/3-octave bands of 500, 1000 and 2000 Hz, and the theoretical lines at the center and upper/lower cutoff frequencies. Although some discrepancies are seen in the 500 Hz band, the measured results well correspond with the theoretical ones regardless of the type of porous materials. It is noted that theoretical absorption coefficients around 70 degrees are considerably sensitive to the parameters estimated under the normal-incidence condition, and furthermore, the effect of anisotropy will be included in the measured results.

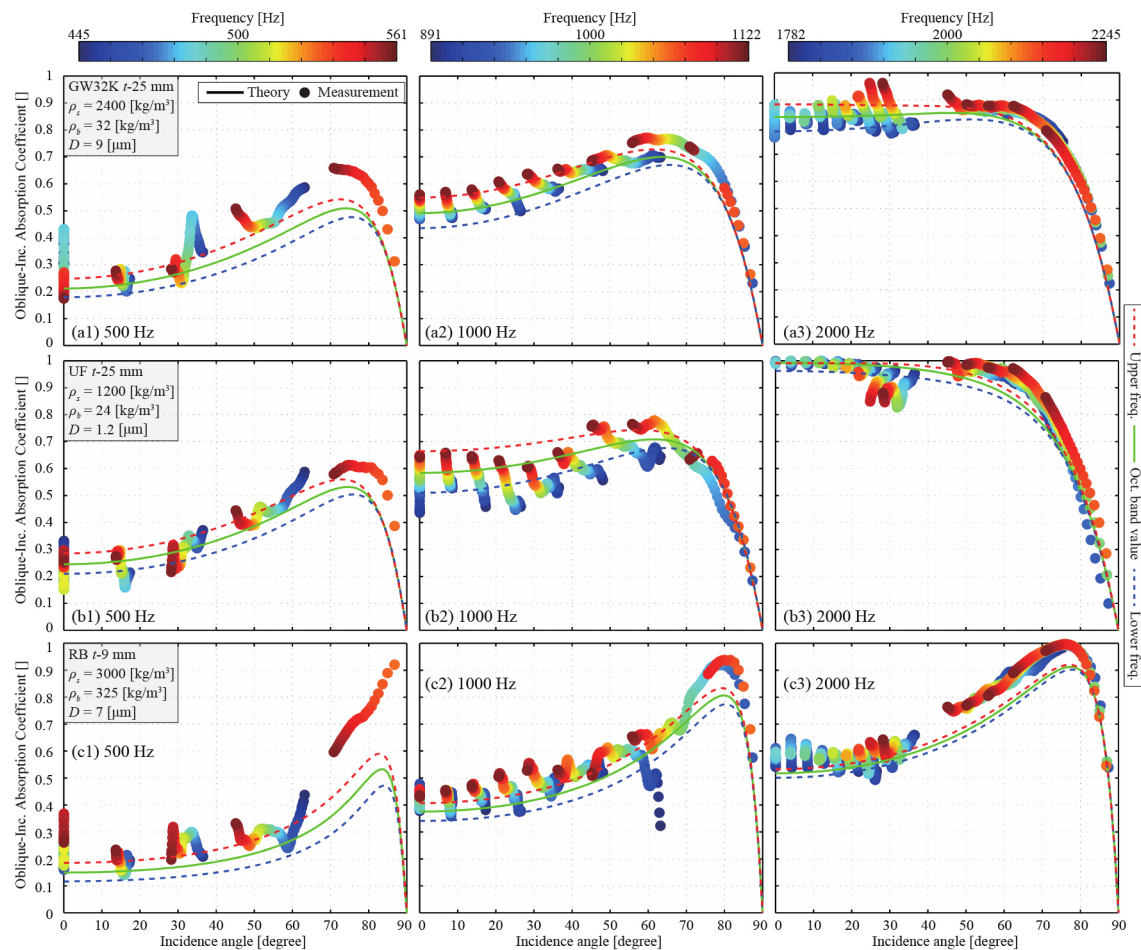


Figure 10 – Oblique-incidence absorption coefficients measured for three porous materials in 1/3-octave bands of 500, 1000 and 2000 Hz: (a) glass wool, (b) urethane foam, (c) rock wool board.

### 4.2 Perforated Panels

In order to examine the incidence angle dependence of absorption coefficient of resonator-type absorbers, measurements are done for two types of perforated panel structure. One is a 5 mm thick board with holes (diameter: 5 mm; pitch: 25 mm) and a 20 mm thick air layer, of which resonance frequency is 750 Hz. The other is a honeycomb resonators panel composed of a 1 mm thick front plate with holes (diameter: 1 mm; pitch: 8 mm), a 18 mm thick core, and a 1 mm thick back plate, of which resonance frequency is 1015 Hz. Figure 11 shows the measured values around 1000 Hz, with theoretical lines estimated by Atalla's model [6]. It is seen that the ordinary perforated panel has strong incidence angle dependence, where a resonance peak shifts with frequency. On the other hand, the honeycomb resonators panel has no incidence angle dependence below 60 degrees, corresponding to the theoretical estimates.

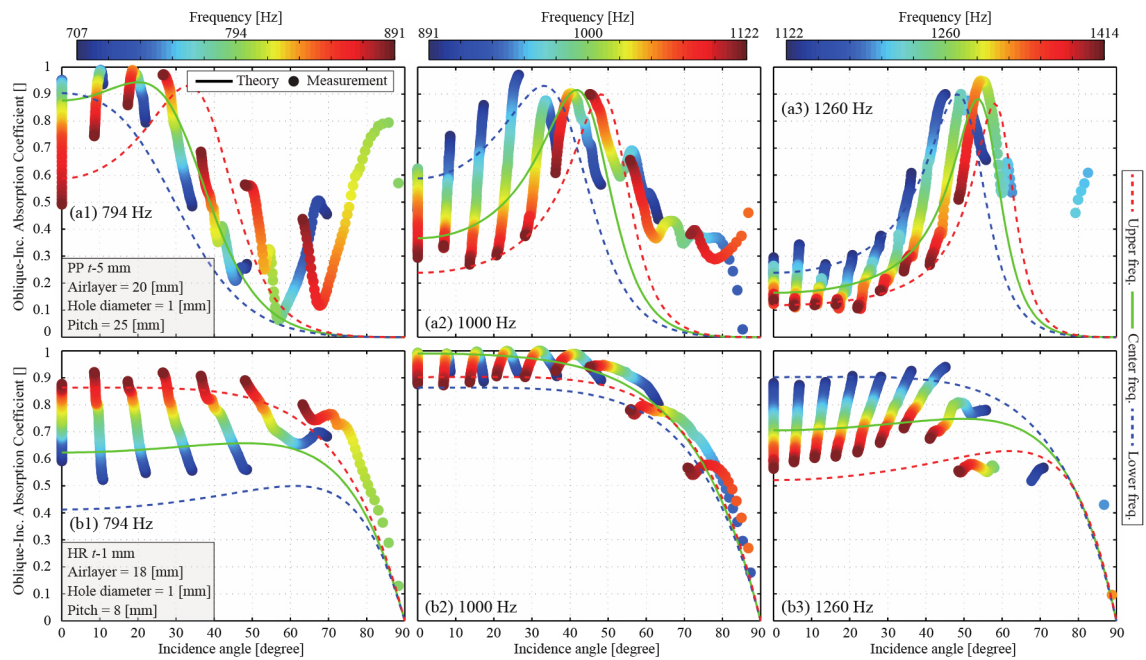


Figure 11 – Oblique-incidence absorption coefficients measured for three porous materials in 1/3-octave bands of 794, 1000 and 1260 Hz: (a) perforated panel, (b) perforated honeycomb panel.

## 5. CONCLUSIONS

The developed thin-chamber system for measuring oblique-incidence absorption coefficients was tested, incorporating two post-processes that exclude the outliers caused by the interval of microphone arrays and the loudspeaker position mismatch. The test measurement for glass wool demonstrated the behavior of the outliers, and confirmed the validity of the two post-processes. Furthermore, using the measured values at all the combinations of frequency and incidence angle, the incidence angle dependence of absorption coefficient was estimated by least squares method. This measurement method was applied for two types of absorbing materials such as porous materials and perforated panels, and their incidence angle dependences were successfully demonstrated in comparison with the theoretical estimates.

## ACKNOWLEDGEMENTS

This project has been funded by the Grant-in-Aid for Challenging Exploratory Research from Japan Society for the Promotion of Science (No. 15K14072).

## REFERENCES

1. Yuzawa M. A method of obtaining the oblique incident sound absorption coefficient through a on-the-spot measurement. *Appl Acoust* 1975;8(1):27-41.
2. Tamura M, Allard JF, Lafarge D. Spatial Fourier-transform method for measuring reflection coefficients at oblique incidence. I: Theory and numerical examples. *J Acoust Soc Am*. 1995;97(4):2255-62.
3. Kimura K, Yamamoto K. A method for measuring oblique incidence absorption coefficient of absorptive panels by stretched pulse technique. *Appl Acoust* 2001;62(6):617-32.
4. Inoue N, Sakuma T. Development of a measurement method for oblique-incidence absorption coefficient using a thin chamber. *Proc 22<sup>nd</sup> ICA*; Buenos Aires, Argentina 2016. No. 421.
5. Kato D. Predictive model of sound propagation in porous material: Extension of applicability in Kato model. *J Acoust Soc Jpn*. 2008;64:339-47.
6. Atalla N, Sgard F. Modeling of perforated plates and screens using rigid frame porous models. *J Sound Vib*. 2007;303:195-208.